

# Retrocyclins Kill Bacilli and Germinating Spores of *Bacillus anthracis* and Inactivate Anthrax Lethal Toxin\*

Received for publication, April 14, 2006, and in revised form, May 30, 2006. Published, JBC Papers in Press, June 21, 2006, DOI 10.1074/jbc.M603614200

Wei Wang<sup>‡</sup>, Chandrika Mulakala<sup>§1</sup>, Sabrina C. Ward<sup>¶</sup>, Grace Jung<sup>‡</sup>, Hai Luong<sup>‡</sup>, Duy Pham<sup>‡</sup>, Alan J. Waring<sup>‡</sup>, Yiannis Kaznessis<sup>§1</sup>, Wuyuan Lu<sup>||</sup>, Kenneth A. Bradley<sup>§</sup>, and Robert I. Lehrer<sup>‡2</sup>

From the Departments of <sup>‡</sup>Medicine and <sup>¶</sup>Microbiology, Immunology, and Molecular Genetics, David Geffen School of Medicine, UCLA, Los Angeles, California 90095, the <sup>§</sup>Department of Chemical Engineering and Materials Science, University of Minnesota, Minneapolis, Minnesota 55455, and the <sup>||</sup>Institute for Human Virology, Biotechnology Institute, University of Maryland, Baltimore, Maryland 21201

$\theta$ -defensins are cyclic octadecapeptides encoded by the modified  $\alpha$ -defensin genes of certain nonhuman primates. The recent demonstration that human  $\alpha$ -defensins could prevent deleterious effects of anthrax lethal toxin *in vitro* and *in vivo* led us to examine the effects of  $\theta$ -defensins on *Bacillus anthracis* (Sterne). We tested rhesus  $\theta$ -defensins 1–3, retrocyclins 1–3, and several analogues of RC-1. Low concentrations of  $\theta$ -defensins not only killed vegetative cells of *B. anthracis* (Sterne) and rendered their germinating spores nonviable, they also inactivated the enzymatic activity of anthrax lethal factor and protected murine RAW-264.7 cells from lethal toxin, a mixture of lethal factor and protective antigen. Structure–function studies indicated that the cyclic backbone, intramolecular tri-disulfide ladder, and arginine residues of  $\theta$ -defensins contributed substantially to these protective effects. Surface plasmon resonance studies showed that retrocyclins bound the lethal factor rapidly and with high affinity. Retrocyclin-mediated inhibition of the enzymatic activity of lethal factor increased substantially if the enzyme and peptide were preincubated before substrate was added. The temporal discrepancy between the rapidity of binding and the slowly progressive extent of lethal factor inhibition suggest that post-binding events, perhaps *in situ* oligomerization, contribute to the antitoxic properties of retrocyclins. Overall, these findings suggest that  $\theta$ -defensins provide molecular templates that could be used to create novel agents effective against *B. anthracis* and its toxins.

Under normal circumstances *Bacillus anthracis* causes human infections only in individuals exposed to infected farm animals or their spore-contaminated products. The virulence of *B. anthracis* primarily derives from the hardness of its spores, an anti-phagocytic capsule that surrounds its vegetative

cells (1), and two secreted binary toxins: lethal toxin (LeTx)<sup>3</sup> and edema toxin (EdTx). Both toxins contain protective antigen (PA, 83 kDa). LeTx also contains lethal factor (LF, 90 kDa), and EdTx contains edema factor (EF, 89 kDa). The genes for all three toxin components, PA, LF, and EF, reside on the pXO1 plasmid (2), and those responsible for capsule synthesis exist on the pXO2 plasmid (3). Both of these plasmids are required for *in vivo* virulence (3).

EF is an adenylate cyclase (4) and LF is a zinc-dependent metalloprotease that selectively attacks certain MAPK kinases (5, 6). PA is required to allow both of the other toxin components to enter host cells (7). When PA binds a cellular receptor (8), it is cleaved into PA63 (63 kDa) and PA20 (20 kDa). The PA20 diffuses away, and the residual receptor-bound PA63 molecules self-associate into ring-shaped heptamers (9) that bind EF or LF with high affinity (10–12). Oligomerization of PA63 leads to endocytosis, which transports the complexes to an acidic compartment (13–15). Here, the heptameric pre-pore changes into an integral-membrane pore (16, 17) that translocates EF or LF into the cytosol (18). Immunization against PA is protective (19).

Defensins are small,  $\beta$ -sheet peptides that collectively possess broad antibacterial, antifungal, and antiviral properties (20–23). They are believed to be especially important as “first responders” to microbial and viral incursions and to play critical roles in defending the mucosal surfaces that line the respiratory, gastrointestinal, and genitourinary tracts. Humans express 6 different  $\alpha$ -defensins and 30 or more  $\beta$ -defensins (24, 25). Human  $\alpha$ -defensins (HNPs) are potent noncompetitive inhibitors of the metalloprotease activity of anthrax LF. They can protect murine macrophages from *B. anthracis* LeTx *in vitro* and provide protection to mice when co-injected with a lethal dose of LeTx (26).

$\theta$ -Defensins are cyclic octadecapeptides that are encoded by mutated  $\alpha$ -defensin genes (27). They have been purified, as peptides, only from the leukocytes and bone marrow of rhesus

\* The work was also supported in part by National Institutes of Health (NIH) Grants AI056921 (to R. I. L.), AI057870 (to K. B.), and AI061482 (to W. L.). The costs of publication of this article were defrayed in part by the payment of page charges. This article must therefore be hereby marked “advertisement” in accordance with 18 U.S.C. Section 1734 solely to indicate this fact.

<sup>1</sup> Supported by NIH Grant GM070989 and by the National Computational Science Alliance (under Grant TG-MCA04T033).

<sup>2</sup> To whom correspondence should be addressed: Dept. of Medicine, David Geffen School of Medicine, UCLA, 10833 LeConte Ave., Los Angeles, CA 90095. Tel.: 310-825-0133; Fax: 310-206-8766; E-mail: rlehrer@mednet.ucla.edu.

<sup>3</sup> The abbreviations used are: LeTx, lethal toxin; EdTx, edema toxin; EF, edema factor; HNP-1, human neutrophil peptide-1 (an  $\alpha$ -defensin); LF, lethal factor; LGA, Lamarckian genetic algorithm; MAPK-2, mitogen-activated protein kinase kinase-2; MEC, minimum effective concentration; PA, protective antigen; RC100<sub>IAA</sub>, reduced and alkylated RC-1; RC-1XX, various retrocyclin analogues; RC-1, retrocyclin-1; RTD, rhesus  $\theta$ -defensin; SPR, surface plasmon resonance; RU, resonance unit(s); BSA, bovine serum albumin; r.m.s.d., root mean square deviation.

**TABLE 1**

**Sequences of the peptides used in this study**

Noncyclic RC-100, the synthetic octadecapeptide precursor of RC-1 (RC-100), contains the three disulfide bonds found in RC-1. Protegrin PG-1, a potentially antimicrobial octadecapeptide originally isolated from porcine leukocytes (66), contains two disulfide bonds.

Name/laboratory ID	Sequence
HNP-1	ACYCRIPACIAGERRYGTCTIYQRLWAFCC
RC-100	cyclic[GICRCICGRGICRCICGR]
<b>Chirality and order</b>	
RC-110	cyclic[RGICRCICGRGICRCICG] (all-D)
RC-111	cyclic[RGICRCICGRGICRCICG] (all-D)
RC-112	cyclic[GICRCICGRGICRCICGR] (all-D)
<b>Arginine substitutions</b>	
RC-100	cyclic[GICRCICGRGICRCICGR]
RC-107G	cyclic[GICRCICGGGICRCICGR]
RC-107GG	cyclic[GICRCICGGGICRCICGG]
RC-107G2H2	cyclic[GICHCICGGGICHICGG]
RC-107G2Ha	cyclic[GICRCICGGGICHICGG]
RC-107G2Hb	cyclic[GICHCICGGGICRCICGG]
RC-101	cyclic[GICRCICGKGICRCICGR]
<b>Retrocyclins versus RTDs</b>	
RC-100	cyclic[GICRCICGRGICRCICGR]
RC-100b	cyclic[GICRCICGRRICRCICGR]
RC-100c	cyclic[RICRCICGRRICRCICGR]
RTD-1	cyclic[GFCRCICRRGVCRICTR]
RTD-2	cyclic[GVCRCICRRGVCRICRR]
RTD-3	cyclic[GFCRCICTRGFCRCICTR]
<b>Cyclic backbone and SS bonds</b>	
Noncyclic RC-100	GICRCICGRGICRCICGR
Reduced and alkylated RC-100	cyclic[GICRCICGRGICRCICGR]
Protegrin PG-1	RGRLCYCRRRFCVGVGR-amide

macaques (28–30), whose three  $\theta$ -defensins are named rhesus  $\theta$ -defensins (RTDs) 1–3. Humans have multiple  $\theta$ -defensin genes, including some that are transcribed. However, human genes and their transcripts contain a premature stop codon that aborts successful translation (27, 31). Retrocyclins 1–3 are synthetic  $\theta$ -defensin peptides, whose structures are based on human multiple  $\theta$ -defensin pseudogenes. Conceptually, they represent peptides last produced by apes whose eventual progeny included gorillas, chimps, and humans. The purpose of this study was to examine the effects of  $\theta$ -defensins on vegetative cells and spores of *B. anthracis* and on the enzymatic and cytotoxic properties of anthrax LF.

**EXPERIMENTAL PROCEDURES**

**Retrocyclin and Other Peptides**

Retrocyclins (31) and HNP-1, -2, and -3 (32) were prepared by solid-phase peptide synthesis as described previously. Peptide concentrations were established by quantitative amino acid analysis (for  $\theta$ -defensins) or by  $A_{280}$  measurement (for HNPs). Table 1 contains the sequence of every peptide used in this study.

**Spore Preparation**

*B. anthracis* (Sterne strain 7702) spores were prepared as described elsewhere (33). Briefly, *B. anthracis* was grown in Trypticase soy broth medium (T8907, Sigma) at 30 °C with constant shaking at 250 rpm for 5–7 days until sporulation. The culture was centrifuged at 6000 × *g* for 20 min at 4 °C. The pellet was resuspended in sterile water, and cultured at 30 °C for two more days with constant shaking to promote further spor-

ulation and bacterial lysis. Complete spore formation was confirmed by light microscopy. Spores were centrifuged at 6000 × *g* for 20 min at 4 °C and washed five times with sterile water. Before use, the spores were heated at 65 °C for 30 min to kill any germinated or germinating spores. No intact bacilli were present at this stage. Serial dilutions of the spore preparation were plated on Trypticase soy agar plates to determine the concentration of colony forming units.

**Radial Diffusion Assay**

Two-stage radial diffusion assays were used to test the antimicrobial activity of peptides against *B. anthracis* spores and vegetative cells (34).

*Stage 1*— $1-4 \times 10^6$  colony forming units were dispersed in a thin 1% agarose underlay gel containing 10 mM phosphate buffer (pH 7.4), 100 mM NaCl, and 1% (v/v) Trypticase soy broth. A 6 × 6 array of wells, each with a 3-mm diameter and 9- $\mu$ l capacity, was punched. Serially diluted peptide solutions containing 250, 79, 25, 7.9, 2.5, and 0.79  $\mu$ g/ml peptides (8  $\mu$ l each) were added to each set of 6 wells. The plate was incubated at 37 °C for 3 h to allow the peptides to diffuse into the underlay gel.

*Stage 2*—An overlay gel containing 60 mg/ml Trypticase soy broth powdered medium plus 1% agarose was poured over the underlay gel, and the plate was incubated overnight to allow surviving bacteria to form micro-colonies. The clear zones around each well were measured 18–24 h later. To determine the minimal effective concentration (MEC), a linear regression function relating the adjusted diameter (zone diameter minus the well diameter) to the log<sub>10</sub> peptide concentration was calculated. The X-intercept defined by this function gives the MEC. Typically, the correlation coefficient ( $r^2$ ) was >0.98.

**Enzymatic Assay**

The enzymatic activity of anthrax lethal factor (LF), a zinc metalloprotease, was measured by monitoring cleavage of a specific substrate by fluorescence resonance energy transfer. The substrate, purchased from Calbiochem, was an internally quenched, *N*-acetylated, *C*-7-amino-4-methylcoumarin derivative of a 14-mer mitogen-activated protein kinase/extracellular signal-regulated-kinase-2 (MEK-2) peptide. Its cleavage by recombinant LF (Calbiochem) resulted in increased fluorescence that was monitored kinetically with an fmax fluorescence microplate reader (Molecular Devices, Sunnyvale, CA), with excitation set at 360 nm and emission at 460 nm. Unless otherwise noted, 100 nM LF was incubated for 30 min at room temperature with the specified amount of  $\theta$ -defensin peptide before 50  $\mu$ M substrate (final concentration) was added.

**Murine Macrophage Intoxication**

Murine macrophage-like RAW 264.7 cells were seeded in 384-well plates at 4000 cells per well and incubated overnight at 37 °C. The medium was replaced by 20  $\mu$ l of fresh Dulbecco's modified Eagle's medium containing 25 mM HEPES, 2 mM glutamine, 100  $\mu$ g (each) penicillin and streptomycin, and 1% fetal bovine serum. The  $\alpha$ - and  $\theta$ -defensin peptides were serially diluted into the same medium, and 20  $\mu$ l was added to appropriate wells. Peptide concentrations

ranged from 0 to 60  $\mu\text{g/ml}$ . LeTx (20  $\mu\text{l}$ ) diluted in fresh media was added to each well giving final concentrations of 100 ng/ml PA and 100 ng/ml LF. Cells were incubated overnight at 37 °C. Cell viability was assayed with the CellTiter-Glo<sup>®</sup> luminescent cell viability kit per the manufacturer's (Promega, Madison, WI) instructions.  $\text{IC}_{50}$  values were obtained with GraphPad Prism Software.

### Ultracentrifugation

Sedimentation equilibrium runs were performed at 25 °C in 12-mm path length double sector cells on a Beckman Optima XL-A analytical ultracentrifuge. Absorption was monitored at 228 nm for 0.1 mg/ml samples and 260 nm for 1.0 mg/ml samples. Peptide samples were in 100 mM NaCl, 10 mM Tris, pH 7.4, and sedimentation equilibrium profiles were measured at 40,000 and 50,000 rpm. The data were initially fitted with a nonlinear least-squares exponential fit for a single ideal species using the Beckman Origin-based software (version 3.01). Preliminary analysis of the association behavior used the global analysis software (the "multifit" option of the abovementioned software) to analyze four scans simultaneously, corresponding to protein at 0.1 mg/ml at 40,000 and 50,000 rpm and protein at 1.0 mg/ml at 40,000 and 50,000 rpm. The partial specific volume (0.711 of RC-1 was calculated from its amino acid composition (35).

### Surface Plasmon Resonance Studies

SPR experiments were performed on a BIAcore 3000 system (BIAcore AB, Uppsala, Sweden). Proteins were immobilized on a BIAcore CM5 sensor chip using the BIAcore amine-coupling protocol. Analytes were introduced into the flow cells in a running buffer containing 10 mM HEPES, pH 7.4, 150 mM NaCl, 3 mM EDTA. The running buffer also contained 0.005% polysorbate-20 to reduce nonspecific binding. Values were corrected for background binding to the CM5 chip. Data were analyzed with BIAevaluation 3.1 software, and curve fitting was done with an assumption of 1:1 binding.

SPR results are expressed in resonance units (RUs). To calibrate the instrument, we synthesized [<sup>14</sup>C]RC-2, which contained [<sup>14</sup>C]glycine (Sigma) and purchased <sup>125</sup>I-bovine serum albumin (BSA) from MP Biomedicals (Irvine, CA). The [<sup>14</sup>C]RC-2 had a specific activity of 21.6  $\mu\text{Ci/mg}$ , and the <sup>125</sup>I-BSA had a specific activity of 987  $\mu\text{Ci/mg}$ . To calibrate the system for BSA, we immobilized a mouse anti-BSA monoclonal antibody (U.S. Biological, Swampscott, MA) on a CM5 biosensor chip. After measuring the binding of <sup>125</sup>I-BSA (1  $\mu\text{g/ml}$ ) to the biosensor chip, the bound analyte was recovered using the BIAcore Analyte Recovery Wizard<sup>®</sup> program, and its radioactivity was measured in a Beckman liquid scintillation spectrometer. From seven such measurements, we determined that 1 RU of BSA was equivalent to  $13.35 \pm 0.55$  pg (mean  $\pm$  S.E.). We used this value to estimate the amount of immobilized LF on the biosensor chip in experiments with retrocyclins. To obtain a conversion factor for RC-2, we used a biosensor that contained immobilized recombinant gp120 (BioDesign International, Saco, ME). From these experiments, we determined that 1 RU corresponded to  $4.41 \pm 0.15$  pg of RC-2 (mean  $\pm$  S.E.,  $n =$

3). We used these values to estimate the stoichiometry with which retrocyclins bound to LF.

### Computational Methods

Docking was accomplished with the AutoDock 3.06 suite of programs (36) which assumes that the macromolecule is rigid, while the ligand is allowed torsional flexibility. A Lamarckian genetic algorithm (LGA) searches the conformational space of the ligand in the vicinity of the macromolecule and ranks the docked molecules on the basis of its binding energy. Also available are two local search methods based on the method of Solis and Wets (37) and an empirical free energy function that estimates the binding free energy (36). In the present work all protein and ligand hydrogen atoms were explicitly modeled, with polar and nonpolar atoms being assigned Lennard-Jones 12-10 and 12-6 parameters, respectively. They were added to the native and ligand complexed forms of anthrax lethal factor (Protein Data Bank designations 1J7N (38), 1PWW (39), and 1YQY) (40) and the ligand (L2) of 1PWW using the WHAT IF web interface (41).

The NMR structures of RTD-1 and retrocyclin (RC)-2 (1HVZ and 2ATG) already had hydrogen atoms. RC-1 was generated by mutating RC-2 *in silico* with Pymol.<sup>4</sup> All water molecules were removed during docking. Partial charges were assigned to the protein atoms using all-atom charges of the AMBER force field (43). Atomic solvation parameters and atomic fragmental volumes were added with the AddSol program of AutoDock 3.06. The Lennard-Jones parameters used for  $\text{Zn}^{2+}$ , taken from the work of Stote and Karplus (44), successfully reproduced the crystal structures of L1 and L2 (Table 4). Hydrogen atoms for the hydroxamate ligand of 1YQY (L1) were added with BABEL,<sup>5</sup> and partial charges were generated with GAMESS (46). Ligand rotatable bonds for all docked ligands were defined using the AutoTors module of AutoDock.

Van der Waals and electrostatic energy grid maps were prepared using AutoGrid (36). These grid maps define the cubic space in the vicinity of receptor in which the search for the optimally binding ligand conformer is focused. The grid points were spaced 0.375 Å apart and based on the centers of L1 and L2, with the grid sized to allow a 5-Å clearance on either side of the ligands in the  $x$ ,  $y$ , and  $z$  dimensions. For RC-2 and RTD-1 two grid sizes were used. The first grid was based on the N terminus MAPKK-2 peptide in complex with anthrax lethal factor (1JKY) (38), which spans the entire active site. This grid was therefore centered on the MAPKK-2 peptide, also with a 5-Å clearance on either side in the  $x$ ,  $y$ , and  $z$  dimensions and a grid spacing of 0.375 Å. Later, when it was found that the RTD-1 and RC-2 docked only in a cavity close to the C-terminal end of the MAPKK-2 peptide in active site, the grid size was reduced to cover only that volume of space to improve the search efficiency. RC-1 was therefore docked using the smaller grid alone. The force-field parameters of AutoDock 2.4 were used to evaluate nonbonded interaction energies instead of using the parameters of AutoDock 3.0, which estimates free energies. This was because the presence of a large number of conforma-

<sup>4</sup> W. L. Delano (2002) The Pymol Molecular Graphics System, www.pymol.org.

<sup>5</sup> P. Walters and M. Stahl (1992) BABEL, smog.com/chem/babel/.

TABLE 2

MEC against vegetative cells and spores of *B. anthracis* (Sterne)Values represent the mean  $\pm$  S.E. The number of determinations (*n*) appears in parentheses.

Peptide name	Short ID	Vegetative cells	Spores
		$\mu\text{g/ml}$	
Human neutrophil peptide-1	HNP-1	$0.85 \pm 0.04$ (3)	$24.9 \pm 0.49$ (3)
RC-1	RC-100	$0.89 \pm 0.03$ (5)	$0.69 \pm 0.05$ (8)
<b>Chirality and residue order</b>			
Retroenantio-RC-1	RC-110	$1.15 \pm 0.06$ (4)	$0.79 \pm 0.00$ (3)
Retro-RC-1	RC-111	$13.6 \pm 2.78$ (3)	$0.32 \pm 0.04$ (3)
Enantio-RC-1	RC-112	$0.99 \pm 0.05$ (4)	$0.51 \pm 0.02$ (3)
<b>Arginine substitutions</b>			
(R <sub>9</sub> G)-RC-1	RC107G	$1.08 \pm 0.04$ (3)	$1.61 \pm 0.084$ (4)
(R <sub>9,18</sub> G)-RC-1	RC107GG	$2.80 \pm 0.06$ (3)	$3.31 \pm 0.525$ (4)
(R <sub>9,18</sub> G, R <sub>13</sub> H)-RC-1	RC107G2Ha	$7.91 \pm 1.02$ (3)	>250 (3)
(R <sub>9,18</sub> G, R <sub>4</sub> H)-RC-1	RC107G2Hb	$24.8 \pm 0.17$ (3)	>250 (3)
(R <sub>9,18</sub> G, R <sub>4,13</sub> H)-RC-1	RC107G2H2	>250 (3)	>250 (3)
<b>Retrocyclins versus RTDs</b>			
RC-2	RC-100b	$0.47 \pm 0.05$ (4)	$0.28 \pm 0.025$ (4)
RC-3	RC-100c	$0.88 \pm 0.03$ (3)	$7.70 \pm 0.64$ (3)
Rhesus $\theta$ -defensin-1	RTD-1	$0.98 \pm 0.05$ (3)	$0.39 \pm 0.018$ (3)
Rhesus $\theta$ -defensin-2	RTD-2	$0.72 \pm 0.05$ (3)	$0.25 \pm 0.02$ (3)
Rhesus $\theta$ -defensin-3	RTD-3	$1.62 \pm 0.24$ (3)	$0.68 \pm 0.03$ (3)
R9K-RC-1	RC-101	$0.32 \pm 0.03$ (4)	$0.58 \pm 0.01$ (4)
<b>Cyclic backbone and SS bonds</b>			
Noncyclic RC-1	RC100ox	$2.31 \pm 0.07$ (3)	$24.9 \pm 0.12$ (3)
Reduced and alkylated RC-1	RC100IAA	>250 (3)	>250 (3)
Protegrin PG-1	PG-1	$1.34 \pm 0.01$ (3)	$1.06 \pm 0.15$ (3)

tional degrees of freedom in the docked ligands presented challenges with the estimation of the torsional free energy term (36). The reported binding energies are therefore representative of binding enthalpies and not binding free energies. Electrostatic interactions were evaluated using a distance-dependent dielectric constant to model solvent effects.

For the global search using the LGA, the size of the initial random population was 200 individuals for the large grids and 50 individuals otherwise, the maximal number of energy evaluations was  $2 \times 10^7$ , the maximal number of generations was 500, the number of top individuals that survived into the next generation, the elitism, was 1, the probability that a gene would undergo a random change was 0.02, the crossover probability was 0.80, and the average of the worst energy was calculated over a window of ten generations.

For a pure local search, the pseudo-Solis and Wets method was used, whereas the Solis and Wets method was used for the LGA part of the local search. The parameters used for local search in both cases were a maximum of 1000 iterations per local search, the probability of performing a local search on an individual was 1.0, the maximal number of consecutive successes or failures before doubling or halving the step size of the local search was 4, and the lower bound on the step size, 0.01, was the termination criteria for the local search. For RTD-1 and RC-2, a total of 50 dockings was performed using the large grid before switching to the smaller grid. For the root-mean squared deviation (r.m.s.d.) calculation of docked of L1 and L2, their crystal coordinates were used as reference.

## RESULTS

**Activity against Spores and Bacilli**—We used the capsule-deficient Sterne strain of *B. anthracis* to examine the antimicrobial activity of retrocyclins. Radial diffusion and colony counting assays were performed in the presence of physiologi-

cal NaCl concentrations. Table 2 summarizes the results of our radial diffusion assays, which showed that RC-1 and HNP-1 killed vegetative *B. anthracis* cells with an MEC  $< 1 \mu\text{g/ml}$ . Retrocyclin-1 also manifested this exceptional potency against *B. anthracis* spores, but HNP-1 did not (MEC  $24.9 \pm 0.49 \mu\text{g/ml}$ ). Because RC-112, an all D-amino acid version of RC-1, and RC-110, a retroenantio version of RC-1 were as effective as the regular peptide, chiral interactions were apparently not required for antimicrobial activity. RC-111, the retro analog of RC-1, showed reduced activity against vegetative cells (MEC  $13.6 \pm 2.78 \mu\text{g/ml}$ ) but had excellent activity against spores (MEC  $0.32 \pm 0.04 \mu\text{g/ml}$ ).

Table 2 also contains structure-function data.  $\theta$ -Defensins possess a cyclic peptide backbone and three intramolecular disulfide bonds. RC-100ox, the immediate synthetic precursor of RC-1, contains the three disulfide bonds but has free amino and C termini. This peptide was  $\sim 3$ -fold less potent than cyclic RC-1 against vegetative *B. anthracis* bacteria, and  $\sim 36$ -fold less effective against *B. anthracis* spores. RC-100<sub>IAA</sub> was derived from RC-1 by reducing its disulfide bonds with dithiothreitol and alkylating the liberated cysteine residues with iodoacetamide. RC-100<sub>IAA</sub> thereby retained the net charge (+4) and cyclic peptide backbone of RC-1 but lacked its internal tri-disulfide scaffold. RC100<sub>IAA</sub> lacked activity (MEC  $> 250 \mu\text{g/ml}$ ) against vegetative cells and spores of *B. anthracis* (Sterne). Thus, both the cyclic backbone and the tri-disulfide ladder contributed to activity against *B. anthracis*.

In addition to its six cysteine residues, Retrocyclin-1 contains four residues each of arginine, isoleucine, and glycine. To assess the contribution of the arginines to its activity against *B. anthracis* (Sterne), we synthesized analogs in which 1, 2, 3, or 4 of these arginines were replaced by a glycine and/or a histidine residue. Replacing one (RC-107G) or both (RC-107GG) argi-

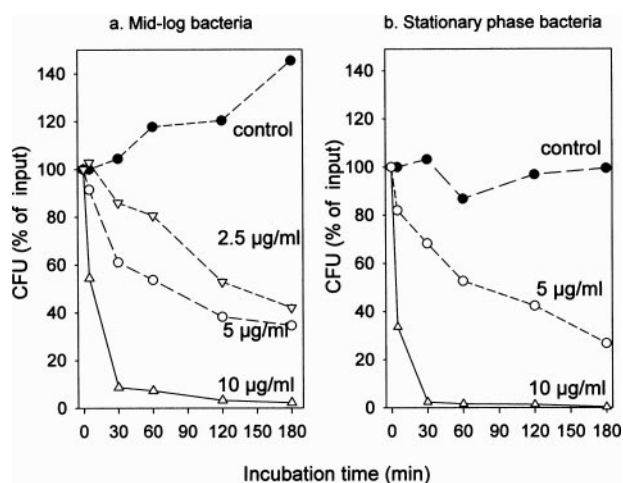


FIGURE 1. **Colony count assays.** Mid-logarithmic (a) and stationary phase (b) *B. anthracis*, Sterne strain bacteria were killed with similar kinetics by RC-2 (RC-100b).

nine residues in the  $\beta$ -turn region(s) of RC-1 had relatively little effect on activity against vegetative cells or spores (Table 2). However, replacing all four arginines (RC-107G2H2) abolished activity (MEC > 250  $\mu\text{g/ml}$ ). When we replaced three arginines (RC-107G2Ha and RC-107G2Hb), this abolished activity against *B. anthracis* spores (MEC > 250  $\mu\text{g/ml}$ ), but activity against vegetative cells persisted (MEC  $7.91 \pm 1.02$  and  $24.8 \pm 0.17$   $\mu\text{g/ml}$ ). Analogs of RC-2 containing a lysine instead of an arginine at position 4, 9, 10, 13, or 18 of RC-2 killed vegetative *B. anthracis* cells with a MEC < 1  $\mu\text{g/ml}$ , as did an analog in which both Arg-9 and Arg-10 were replaced by lysines (data not shown).

We also examined activity against vegetative cells of *B. anthracis* (Sterne) in colony count assays. Fig. 1 shows that mid-logarithmic and stationary phase organisms showed similar susceptibility to RC-2 and that its bactericidal activity was time- and concentration-dependent. In contrast, when we used colony count assays to test activity against *B. anthracis* (Sterne) spores, we saw no decrease in colony forming units/ml after 3 h of incubation with 25  $\mu\text{g/ml}$  RC-2 (data not shown). This suggests that the potent activity of RC-2 against *B. anthracis* spores seen in our radial diffusion assays (Table 2) was exerted after the spores had commenced to germinate, rather than against quiescent spores.

**Effect on Enzymatic Activity**—Anthrax LF is a highly substrate-specific  $\text{Zn}^{2+}$ -metalloprotease. Table 3 summarizes the ability of 16 different  $\theta$ -defensins to inhibit the enzymatic activity of LF. The tested peptides included RC-1 (RC-100) and its retro (RC-111), enantio (RC-112), and retroenantio (RC-110) analogs. Although these peptides were similar in composition, net charge, and sequence, the retro (RC-111) and enantio (RC-112) analogs were only half as potent as RC-1, and the retroenantio analog (RC-110) was  $\sim 25\%$  as effective. Thus, chirality and polarity relative to the peptide backbone also contributed to the ability to inactivate LF. The cyclic backbone was extremely important, because the  $\text{IC}_{50}$  of RC-100ox (the  $\beta$ -hairpin, noncyclic synthetic precursor of RC100) was increased 5-fold relative to RC-1.

TABLE 3

**Inhibition of the enzymatic activity of anthrax LF**

Data, shown as, are mean  $\pm$  S.E. values from at least three independent experiments with each peptide.  $\text{IC}_{50}$  values for each peptide were compared to those obtained for RC-1 by unpaired *t* test.

Peptide	Laboratory name	Mean $\text{IC}_{50} \pm$ S.E.
		$\mu\text{g/ml}$
RC-1	RC-100	$4.23 \pm 0.82$
Retroenantio-RC-1	RC-110	$19.9 \pm 2.01^a$
Retro-RC-1	RC-111	$7.73 \pm 0.29^b$
Enantio-RC-1	RC-112	$9.37 \pm 1.21^b$
<b>Retrocyclins versus RTDs</b>		
RC-1	RC-100	$4.98 \pm 0.88$
RC-2	RC-100b	$3.60 \pm 0.23$
RC-3	RC-100c	$11.1 \pm 2.15^b$
Rhesus $\theta$ -defensin-1	RTD-1	$5.13 \pm 0.48$
Rhesus $\theta$ -defensin-2	RTD-2	$7.93 \pm 1.41$
Rhesus $\theta$ -defensin-3	RTD-3	$4.70 \pm 0.60$
<b>Arginine substitutions</b>		
RC-1	RC-100	$4.23 \pm 0.82$
(R <sub>9</sub> G)-RC-1	RC107G	$5.63 \pm 0.49$
(R <sub>9,18</sub> G)-RC-1	RC107GG	$9.25 \pm 0.95^b$
(R <sub>9,18</sub> G, R <sub>13</sub> H)-RC-1	RC107G2Ha	$9.43 \pm 0.43^a$
(R <sub>9,18</sub> G, R <sub>4</sub> H)-RC-1	RC107G2Hb	$12.9 \pm 2.23^b$
(R <sub>9,18</sub> G, R <sub>4,13</sub> H)-RC-1	RC107G2H2	>50 <sup>a</sup>
<b>Cyclic backbone and SS bonds</b>		
Noncyclic RC-1	RC100ox	$22.7 \pm 5.79^b$
Reduced and alkylated RC-1	RC100 <sub>1AA</sub>	>50 <sup>a</sup>
Protegrin PG-1	PG-1	$14.8 \pm 2.41^b$
Human neutrophil peptide-1	HNP-1	$6.58 \pm 1.48$

<sup>a</sup>  $p < 0.01$ .

<sup>b</sup>  $p < 0.05$ .

Replacing one  $\beta$ -turn arginine residue with glycine (RC-107G) had slight effect on potency, but replacing two of them (RC-107GG) reduced potency 2-fold. Further replacement of a single  $\beta$ -sheet arginine with histidine (RC-107G2Ha and RC-107G2Hb) caused little further impairment, but replacing both of these arginines with histidines (RC-107G2H2), abolished it completely. These findings suggest that the arginines may operate in a pairwise fashion with respect to inhibiting the enzymatic activity of LF. Placing a lysine instead of an arginine at position 4, 9, 10, 13, or 18 of RC-2 neither enhanced nor diminished inhibitory activity against LF (data not shown).

Retrocyclins 1–3 and RTDs 1–3 had fairly similar potency (Table 3). Although RC-2 appeared somewhat more effective than RC-1, the difference was relatively small, and not statistically significant. Retrocyclin-3 was less effective than RC-1 ( $p < 0.05$ ), despite having two additional arginine residues that gave it a net charge of +6 instead of +4. The generally similar activity of the retrocyclins 1–3 and RTD 1–3 suggests that their ability to inhibit LF likely resides in features they all share, namely a cyclic backbone, a conserved tri-disulfide ladder, and certain arginine residues.

**Effect of Preincubation**—Fig. 2a shows that by preincubating LF with retrocyclin, inhibition of the enzymatic activity of the toxin was considerably enhanced. In the absence of preincubation, 2.5  $\mu\text{M}$  RC-1 inhibited enzymatic activity by  $\sim 20\%$ . Inhibition increased to 40% after a 5-min preincubation, to 60% after 15-min preincubation, and to 80% after a 30-min preincubation. In Table 3, inhibition was measured after a 30-min preincubation between recombinant LF and the indicated  $\theta$ -defensin. Fig. 2b shows that increasing the substrate concentration did not reverse the inhibition of LF by RC-2, clearly indicating

## Retrocyclins and the Anthrax bacillus

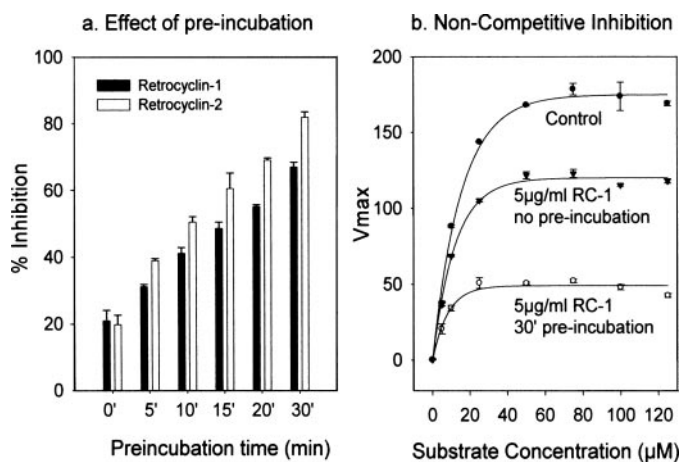


**FIGURE 2. Characteristics of inhibition.** *a*, inhibitory effect of 5  $\mu\text{g}/\text{ml}$  retrocyclins 1 and 2 on LF. Inhibition by retrocyclins increased progressively as the duration of preincubation with LF was prolonged. *b*, maximal rate of substrate hydrolysis ( $V_{\text{max}}$ ) by 100 nM LF, with or without a 30-min preincubation with 5  $\mu\text{g}/\text{ml}$  RC-1. Substrate concentrations varied from 5 to 120  $\mu\text{M}$ . *b*, effects of preincubation and of substrate concentration on  $V_{\text{max}}$ . The respective  $K_m$  values, estimated graphically, were as follows: control, 10.7  $\mu\text{M}$ ; 30-min preincubation, 8.5  $\mu\text{M}$ ; no preincubation, 5.8  $\mu\text{M}$ .

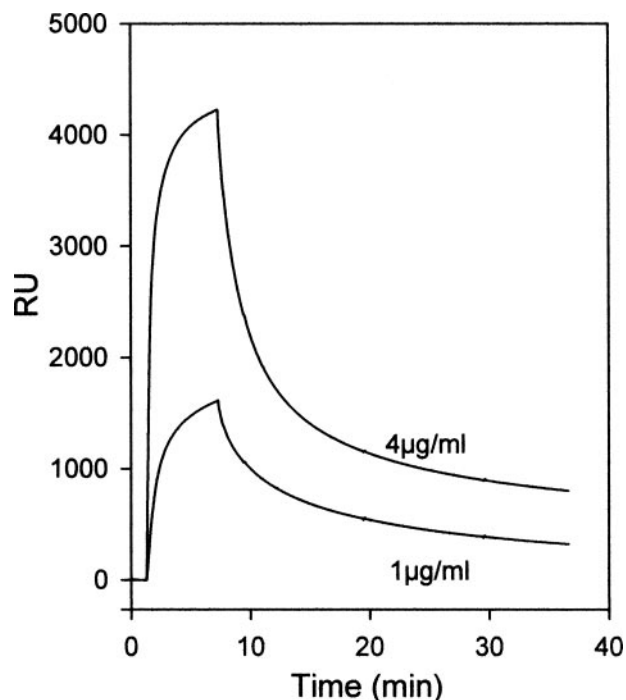


**FIGURE 3. Binding kinetics.** Binding of RC-1 to LF was examined by SPR. The biosensor was a CM5 chip containing 4422 resonance units ( $\sim 50$  ng) of immobilized anthrax LF. Binding isotherms for 1 and 4  $\mu\text{g}$  of retrocyclin/ml are shown.

that the process was not competitive. The  $V_{\text{max}}$  of RC-treated LF was considerably reduced, consistent with noncompetitive inhibition, and the  $K_m$  was also reduced, from  $\sim 10$   $\mu\text{M}$  to  $\sim 5$   $\mu\text{M}$ , consistent with uncompetitive inhibition.

**Kinetics of Binding**—We used SPR to examine the binding of RC-1 to immobilized anthrax LF (Fig. 3). Binding isotherms are shown for two concentrations of RC-1: 4  $\mu\text{g}/\text{ml}$  ( $\sim 2$   $\mu\text{M}$ ) and 1  $\mu\text{g}/\text{ml}$  ( $\sim 0.5$   $\mu\text{M}$ ). Binding was rapid, with maximal binding reached after  $\sim 5$  min. From these isotherms and others

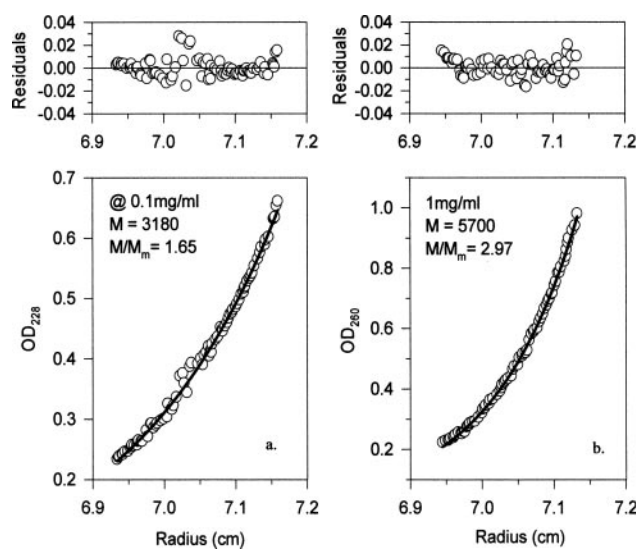


**FIGURE 4. Oligomerization of RC-1.** Analytical ultracentrifugation was done at two different initial peptide concentrations. At 100  $\mu\text{g}/\text{ml}$  (*a*), retrocyclin migrated as a mixture of monomers and dimers. At 1 mg/ml (*b*), trimers predominated.

obtained at lower retrocyclin concentrations, the following constants were calculated for the binding of RC-1 to LF:  $k_{\text{on}}$ ,  $1.99 \times 10^4$ ;  $k_{\text{off}}$ ,  $1.51 \times 10^{-3}$ ;  $K_d$ , 79.1 nM.

SPR experiments provide a readout in resonance units. To convert RUs to mass-based quantities, we performed experiments with [ $^{14}\text{C}$ ]RC-2 and [ $^{125}\text{I}$ ]BSA. From the former, we determined that 1 RU of RC-2 corresponded to  $4.42 \pm 0.25$  pg (mean  $\pm$  S.E.,  $n = 3$ ). For [ $^{125}\text{I}$ ]BSA, we determined that 1 RU was equivalent to  $13.35 \pm 0.55$  pg of protein (mean  $\pm$  S.E.,  $n = 7$ ). If we apply the same RU/pg conversion factors to RC-1 and LF, respectively, the following estimates result. The 4422 RUs of LF affixed to the biosensor chip represents  $\sim 59.0$  ng (or 0.66 pmol) of this toxin. When the biosensor was exposed to 4  $\mu\text{g}/\text{ml}$  RC-1,  $\sim 4000$  RU of the defensin was bound (Fig. 3). This corresponds to 17.7 ng or  $\sim 9.23$  pmol of retrocyclin. Thus, each LF molecule bound  $\sim 14$  molecules of retrocyclin. At 1  $\mu\text{g}/\text{ml}$ , when  $\sim 1500$  RU of retrocyclin was bound, the molar ratio was 5.25 retrocyclins/LF.

The different kinetics of binding (rapid) and protease inhibition (slowly progressive) suggest that one or more post-binding steps may be responsible for the time-dependent nature of the inhibition of the enzymatic activity of LF shown in Fig. 2*a*. One post-binding event that could contribute to the progressive enzymatic inactivation is illustrated in Fig. 4, which shows that RC-1 can oligomerize to form dimers or trimers. SDS-PAGE analysis also demonstrated this property (data not shown).

**Prevention of Cellular Intoxication**—The ability of  $\alpha$ - and  $\theta$ -defensins to protect RAW 264.7 cells from intoxication by LeTx, a mixture of PA and LF, is illustrated in Fig. 5. Fig. 5*a* confirms the protective activity of HNP-1, which had an  $\text{IC}_{50}$  of  $\sim 5.5$   $\mu\text{g}/\text{ml}$  in this experiment. We obtained similar results in a second experiment (data not shown). Fig. 5*b* shows that RC-1 and -2 were also protective, acting with an  $\text{IC}_{50}$  between 5.5 and 7.0  $\mu\text{g}/\text{ml}$ . Fig. 5*c* shows that RC-112, composed exclusively of D-amino acids, was about half as potent as RC-1, its enantiomer, acting with an  $\text{IC}_{50}$  of  $\sim 15$   $\mu\text{g}/\text{ml}$ . This panel also shows that

RC110, the retroenantio analog of RC-1, had very little protective activity even though its net charge and composition mirrored that of RC-1. The results shown in Fig. 5 (b and c) are representative of four individual experiments, each done with triplicate samples.

**Docking Studies**—Docking was performed on three crystal forms of LF: 1J7N, native LF (38); 1YQY, LF complexed with a potent hydroxamate inhibitor, L1, with an  $IC_{50}$  value of 60 nM (39); and 1PWW, LF with a nanopptide fragment, L2, in its active site (40). The docking results are summarized in Table 4 with the final docked energy listed for the best docked ligands. In AutoDock, the docked energy is the sum of nonbonded ligand-receptor intermolecular energy and the nonbonded internal energy of the ligand (Table 4). L1 and L2 were docked as controls, and successfully reproduce the crystal structures in local searches with energies of  $-118.8$  kcal/mol and  $-274.32$  kcal/mol and r.m.s.d. values of 0.75 and 0.57 Å from their crystal coordinates, respectively, thus verifying the parameters used for  $Zn^{2+}$ . A global search for L1 turned up a conformation with even lower energy than the local search with a docked energy of  $-123.67$  kcal/mol and an r.m.s.d. of 0.87 Å, showing the effectiveness of the LGA of AutoDock. A global search for L2, however, performs suboptimally, with an energy of  $-254.71$  kcal/mol whose r.m.s.d. is 5.97 Å from its crystal form. This is due to the large number of conformational degrees of freedom in L2.

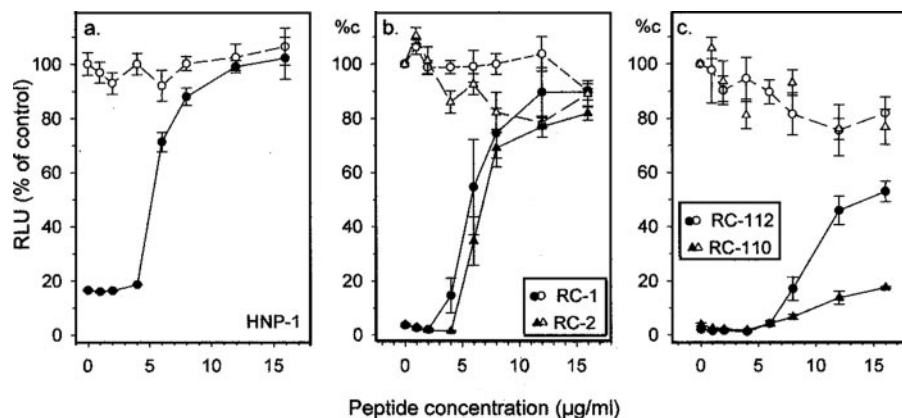


FIGURE 5. **Protection from anthrax LeTx.** RAW264.7 cells were incubated with LeTx and various concentrations of retrocyclin-1 (RC-1), retrocyclin-2 (RC-2), enantio-RC-1 (RC-112), and retroenantio-RC-1 (RC-110) in the presence (solid symbols) or absence (open symbols) of anthrax LeTx, as described in the text. On the following day, target cell survival was estimated by measuring their ATP content with a luciferase assay. These results have been normalized relative to the ATP content of control cells incubated without toxins or defensin peptides.

**TABLE 4**  
Results of the computational docking study

Docked molecule	Source ligand	PDB receptor	Search type <sup>a</sup>	No. of atoms	Torsions	Docked energy			r.m.s.d.	No. of docks
						Internal	Intermolecular	Overall		
						<i>kcal/mol</i>				
L1	1YQY	1YQY	L	42	8	-17.65	-101.15	-118.80	0.75	200
L1	1YQY	1YQY	G	42	8	-19.44	-104.23	-123.67	0.86	100
L2	1PWW	1PWW	L	193	58	-72.14	-202.18	-274.32	0.57	200
L2	1PWW	1PWW	G	193	58	-109.47	-145.24	-254.71	5.97	200
RC-1	2ATG <sup>b</sup>	1J7N	G	260	44 <sup>c</sup>	-154.29	-148.74	-303.03	—	131
RC-2	2ATG	1J7N	G	277	51 <sup>c</sup>	-142.36	-161.42	-303.78	—	217
RTD-1	1HVZ	1J7N	G	282	51 <sup>c</sup>	-173.99	-167.91	-341.90	—	171

<sup>a</sup>L refers to a local search, and G refers to an LGA-based global search.

<sup>b</sup>RC-1 was generated by an *in silico* mutation on the RC-2 NMR structure.

<sup>c</sup>Includes only side-chain torsional degrees of freedom. The circular peptide backbone was kept fixed during docking.

Because AutoDock assumes that the receptor is rigid and torsional flexibility is allowed in the ligand, the degree of flexibility of the ligand determines the computational complexity of the problem. Typical ligands docked with AutoDock usually have less than ten torsional degrees of freedom, whereas L2, even though just a small peptide, has 58 torsional degrees of freedom. Our goal in this modeling work was to dock RTD-1, RC-1, and RC-2, which are octadecapeptides with 44, 51, and 51 torsional degrees of freedom, respectively (after excluding backbone torsional degrees of freedom, because AutoDock cannot model torsional changes in loops). The computational complexity is therefore similar to the computational complexity of L2. However, despite the difficulties in docking outlined with L2, we believe that docking circular peptides with AutoDock may still be feasible, because torsional changes in linear peptides such as L2 would sample much greater conformational space than only side chain perturbations, as would largely be the case with the RTDs and the RCs. Also, to reduce the search space, we focused docking primarily on the active-site cavity, even though the stoichiometry of LF/RC-1 binding as determined by SPR indicates that RC-1 binds to multiple sites on the surface of LF. Our goal was, therefore, to search for RC or RTD binding that would directly interfere with the substrate binding.

Several patterns emerge from our results. When docked in the larger grid (see "Computational Methods"), all RC-2s and RTD-1s docked toward the C-terminal end of MAPKK-2 peptide in the active-site cavity (Fig. 6). It appears that the active site is too narrow toward the N-terminal side to make entry possible from that direction. Access to the active site is, therefore, most likely from the C-terminal side, and for later searches, the grid size was reduced to cover only the C-terminal cavity to make search more efficient.

RC-1 and -2 and RTD-1 dock with energies of  $-303.03$ ,  $-303.78$ , and  $-341.90$  kcal/mol, respectively, which are significantly lower than that of the L2 peptide fragment with the local search, thus implying strong binding may be occurring in

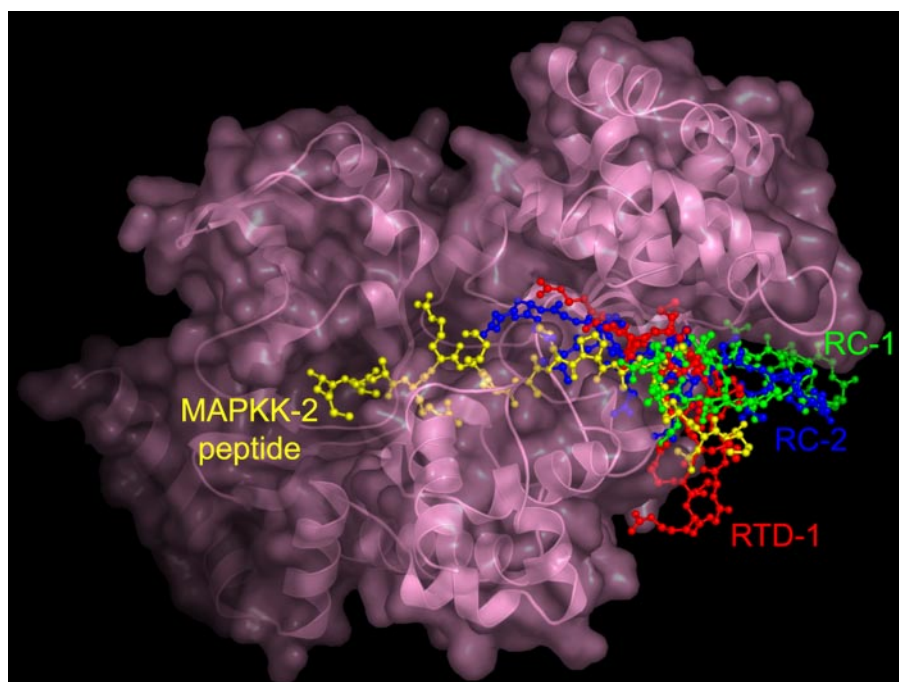


FIGURE 6. Docking of  $\theta$ -defensins to the active site of anthrax lethal toxin. Docked RTD-1 (red), RC-1 (green), and RC-2 (blue) are shown with reference to the N-terminal MAPKK-2 peptide (yellow) in the active-site cavity of anthrax lethal factor.

the active site. Because the docked energies are representative of binding enthalpies and not binding free energies, the trends in their values should be interpreted with care. For instance, even though RTD-1 binds better than RC-2, their NMR structures imply that RTD-1 is more flexible than RC-2. The loss of conformational entropy of the former upon binding, therefore, would be larger when compared with the latter. This needs to be quantified to make an accurate judgment of their relative activities.

In the AutoDock output, the nonbonded interaction of each ligand atom with the receptor is listed. It is therefore possible to determine the contribution of each ligand residue to the intermolecular interaction energy. In the best docks for RTD-1, RC-1, and RC-2 60%, 60, and 62% of the total interaction energy is contributed by the arginines. This is not necessarily surprising because arginines hydrogen bond, besides interacting through electrostatic interactions, and hydrogen bonding energies an order of magnitude larger than van der Waals interactions. In particular, because we have the RC-107 series of mutants available, it is instructive to see the energetic contribution of each of the arginines in RC-1. The energetic contributions in kilocalories/mol of the four arginines are as follows:  $-22.59/R4$ ,  $-0.22/R9$ ,  $-56.75/R13$ , and  $-9.83/R18$ . Keeping in mind the inherent symmetry of RC-1 structure, these energies correlate well with the observed inhibition of RC-1, RC-107G, and RC-107GG toward LF. For example,  $R_9G$  hardly affects the  $IC_{50}$ , but  $R_{9,18}G$  almost doubles it (Table 3).

The stoichiometry of RC-1 binding suggests that the binding is far from specific and that there are several binding sites on the enzyme surface. Docked RTD-1, RC-1, and RC-2, each of which probably represent one of several possible binding modes, show significant overlap with the N-terminal MAPKK-2 peptide

binding site (Fig. 6) implying that they all compete for the same binding site, which contradicts the noncompetitive binding curves observed (Fig. 2*b*). However, the  $k_{off}$  indicates that the half-life of the binding is  $\sim 7.6$  min ( $0.69302/k_{off}$ ), implying the RC-1 binding can be practically considered irreversible compared with substrate binding, if the latter is assumed to be diffusion-limited. Such irreversible binding within the active site should also give noncompetitive binding curves of the sort observed (Fig. 2*b*), because the irreversibly bound inhibitor would reduce the effective concentration of the active enzyme. Also, because the RCs self-aggregate, the slow onset of inhibition observed (Fig. 2*a*) can be explained as follows: once the enzyme surface is covered with RCs, these bound RCs may form nucleation sites for aggregation and compete with the

binding to the active site itself, thus resulting in the slow onset of inhibition.

## DISCUSSION

In nonhuman primates, such as rhesus macaques,  $\theta$ -defensins are encoded by genes that encode a C-terminal "defensin" domain containing 12 residues, including 3 cysteines. Rhesus leukocytes trim and splice two such precursors into a cyclic, 18-residue,  $\theta$ -defensin peptide. The human  $\theta$ -defensin genes contain a premature stop codon, and humans lack  $\theta$ -defensin peptides. Although the sequences of retrocyclins 1, 2, and 3 are based on human genome sequences, these peptides and their analogs were prepared by solid-phase chemical synthesis for this study.

Surprisingly few studies of  $\theta$ -defensin peptides have appeared since their initial description by Selsted *et al.* in 1999 (29), despite their novel characteristics and potential usefulness. Whereas many cyclic peptides are produced by plants, bacteria, or fungi,  $\theta$ -defensins are the only known cyclic peptides of animal origin (47–49). The ability of  $\theta$ -defensins to bind carbohydrates (50) also makes them the smallest known lectins. Their broad antiviral spectrum encompasses human immunodeficiency virus type 1, influenza A, and herpes simplex viruses (31, 51, 52), and its mechanisms have been the focus of many of our recent studies.

$\theta$ -Defensins were reported to kill some bacteria, but not others (29, 30, 53, 54). The present studies show that *B. anthracis* is highly susceptible to their antibiotic effects. Our studies were stimulated by a recent report of Kim *et al.* (26), showing that HNP-, a human  $\alpha$ -defensin, inhibited the enzymatic activity of anthrax LF in a noncompetitive manner. We confirmed this observation for HNP-1 and extended it by showing that  $\theta$ -defensins also inhibit LF in a noncompetitive manner (Fig. 2).

Both  $\theta$ -defensins (Table 2) and HNP-1 (26) required intact disulfide bonds for this activity. On a molar basis, HNP-1 (3.4 kDa) and retrocyclins 1 and 2 (~2 kDa) have similar molar potencies against LF, although retrocyclins are more active on a weight basis (Table 3).

HNP-1 and RC-2 were equally active against *B. anthracis* (Sterne) bacilli (Table 2). In killing *B. anthracis* bacilli (Fig. 1) and inactivating the enzymatic activity of LF (Fig. 2),  $\theta$ -defensins manifested a lag. With respect to the former, we speculated that this delay may have resulted from a requirement for oligomer formation in or near the active site of LF. Oligomerization could also contribute to the delayed onset of killing.

Many, but not all, antimicrobial peptides target the bacterial membrane by binding to it, altering its permeability and dissipating its trans-membrane electrochemical gradient. A relatively thick peptidoglycan wall, the murein sacculus, surrounds the membrane of a Gram-positive bacillus and protects it from destructive osmotic surges. Using fluorescein-labeled dextrans, Demchick and Koch (55) found that the murein sacculi of *Escherichia coli* and *B. subtilis* contain myriads of pores ("tesserae"), each formed by two octasaccharide chains that were cross-linked by two octapeptides. The effective diameter of the pores was ~41 Å, sufficiently large to allow the free passage of a 25-kDa globular hydrophilic molecule. Consequently, the thick peptidoglycan wall surrounding *B. anthracis* is unlikely to impede the transmural journey of  $\theta$ -defensins to destinations in the bacterial membrane or beyond.

In radial diffusion experiments, HNP-1 and  $\theta$ -defensins were active against *B. anthracis* spores, but the  $\theta$ -defensins were far more potent than HNP-1 (Table 2). The reason(s) for this difference remain to be elucidated. Because RC-1 and its all-D-amino acid enantiomer, RC-112 had very similar MECs against *B. anthracis* cells and spores in radial diffusion assays (Table 2), chiral interactions between  $\theta$ -defensins and this organism are unlikely to contribute significantly to the bactericidal mechanism. This contrasts with the inhibition of LF (Table 3). Here, RC-112 was significantly ( $p < 0.05$ ) less effective than RC-1, suggesting that chiral interactions or relatively subtle structural factors have significant effects on the ability to inhibit this toxic metalloprotease.

Mayer-Scholl *et al.* (56) found that human neutrophils phagocytize (ingest) *B. anthracis* bacilli and spores and kill them via an oxygen-independent mechanism that uses  $\alpha$ -defensins as its effectors. Neutrophils sequester ingested bacteria and spores in small membrane-bounded cytoplasmic vacuoles ("phagosomes") and deliver the contents of their defensin-containing "azurophil" storage granules to these phagosomes, achieving local defensin concentrations hundreds of times greater than the MEC of 24.9  $\mu\text{g}/\text{ml}$  shown in Table 2 (57, 58).

Biophysical techniques, including oriented CD, x-ray diffraction, and solid-state NMR, have provided valuable insights into the effects of PG-1 and  $\theta$ -defensins on membranes (42, 59–64). Solid-state NMR studies with uniaxially oriented phosphatidylcholine bilayers revealed that RTD-1 bound to the surface of such bilayers without perturbing its hydrophobic core (64). In contrast, when RTD-1 bound bilayers containing phosphatidylcholine and phosphatidylglycerol lipids, it induced much greater orientational disorder, consistent with its selectivity for

anionic bacterial membranes versus cholesterol-rich zwitterionic mammalian membranes. RTD-1 induced curvature stress and micrometer-diameter lipid cylinders in anionic membranes. In all of these structural and dynamic features, the behavior of membrane-associated RTD-1 differed significantly from that of PG-1 (64). Protegrin PG-1, a noncyclic  $\beta$ -sheet peptide octadecapeptide found in porcine neutrophils (45), was also highly effective against *B. anthracis* spores. However, PG-1 manifests appreciable cytotoxicity, and the peptide is hemolytic for human erythrocytes. In marked contrast,  $\theta$ -defensins such as RC-2 are nonhemolytic and noncytotoxic, even when tested at high concentrations (52).

A dangerous and very often lethal form of human anthrax occurs following the inhalation of aerosolized *B. anthracis* spores. We have shown that certain  $\theta$ -defensins not only exert potent antibiotic activity against the spores and bacilli of *B. anthracis*, they can also inactivate LF and protect cells from destruction by anthrax lethal toxin (LF plus PA). These findings suggest that  $\theta$ -defensins provide molecular templates that could be used to create novel agents effective against *B. anthracis* and its toxins. Kim *et al.* (26) reported that BALB/c mice treated intravenously with 500  $\mu\text{g}$  of mixture of human  $\alpha$ -defensins (HNPs) 1–3 survived a dose of anthrax LeTx that killed untreated mice by Day 2. That an intravenous dose of this magnitude (20 mg/kg) was tolerated and effective is a strong incentive to pursue similar *in vivo* studies with  $\theta$ -defensins.

*Acknowledgment*—We thank Dr. David J. Banks for his help with the spore preparations.

## REFERENCES

- Green, B. D., Battisti, L., Koehler, T. M., Thorne, C. B., and Ivins, B. E. (1985) *Infect. Immun.* **49**, 291–297
- Okinaka, R. T., Cloud, K., Hampton, O., Hoffmaster, A. R., Hill, K. K., Keim, P., Koehler, T. M., Lamke, G., Kumano, S., Mahillon, J., Manter, D., Martinez, Y., Ricke, D., Svensson, R., and Jackson, P. J. (1999) *J. Bacteriol.* **181**, 6509–6515
- Collier, R. J., and Young, J. A. (2003) *Annu. Rev. Cell Dev. Biol.* **19**, 45–70
- Leppla, S. H. (1982) *Proc. Natl. Acad. Sci. U. S. A.* **79**, 3162–3166
- Duesbery, N. S., Webb, C. P., Leppla, S. H., Gordon, V. M., Klimpel, K. R., Copeland, T. D., Ahn, N. G., Oskarsson, M. K., Fukasawa, K., Paull, K. D., and Vande Woude, G. F. (1998) *Science* **280**, 734–737
- Vitale, G., Pellizzari, R., Recchi, C., Napolitani, G., Mock, M., and Montecucco, C. (1998) *Biochem. Biophys. Res. Commun.* **248**, 706–711
- Gordon, V. M., Klimpel, K. R., Arora, N., Henderson, M. A., and Leppla, S. H. (1995) *Infect. Immun.* **63**, 82–87
- Bradley, K. A., Mogridge, J., Mourez, M., Collier, R. J., and Young, J. A. (2001) *Nature* **414**, 225–229
- Milne, J. C., Furlong, D., Hanna, P. C., Wall, J. S., and Collier, R. J. (1994) *J. Biol. Chem.* **269**, 20607–20612
- Cunningham, K., Lacy, D. B., Mogridge, J., and Collier, R. J. (2002) *Proc. Natl. Acad. Sci. U. S. A.* **99**, 7049–7053
- Mogridge, J., Cunningham, K., Lacy, D. B., Mourez, M., and Collier, R. J. (2002) *Proc. Natl. Acad. Sci. U. S. A.* **99**, 7045–7048
- Mogridge, J., Cunningham, K., and Collier, R. J. (2002) *Biochemistry* **41**, 1079–1082
- Beauregard, K. E., Collier, R. J., and Swanson, J. A. (2000) *Cell Microbiol.* **2**, 251–258
- Friedlander, A. M. (1986) *J. Biol. Chem.* **261**, 7123–7126
- Gordon, V. M., Leppla, S. H., and Hewlett, E. L. (1988) *Infect. Immun.* **56**, 1066–1069

16. Blaustein, R. O., Koehler, T. M., Collier, R. J., and Finkelstein, A. (1989) *Proc. Natl. Acad. Sci. U. S. A.* **86**, 2209–2213
17. Milne, J. C., and Collier, R. J. (1993) *Mol. Microbiol.* **10**, 647–653
18. Wesche, J., Elliott, J. L., Falnes, P. O., Olsnes, S., and Collier, R. J. (1998) *Biochemistry* **37**, 15737–15746
19. Friedlander, A. M., Welkos, S. L., and Ivins, B. E. (2002) *Curr. Top. Microbiol. Immunol.* **271**, 33–60
20. Ganz, T. (2004) *C. R. Biol.* **327**, 539–549
21. Lehrer, R. I. (2004) *Nat. Rev. Microbiol.* **2**, 727–738
22. Selsted, M. E., and Ouellette, A. J. (2005) *Nat. Immunol.* **6**, 551–557
23. Lehrer, R. I., Lichtenstein, A. K., and Ganz, T. (1993) *Annu. Rev. Immunol.* **11**, 105–128
24. Scheetz, T., Bartlett, J. A., Walters, J. D., Schutte, B. C., Casavant, T. L., and McCray, P. B., Jr. (2002) *Immunol. Rev.* **190**, 137–145
25. Schutte, B. C., Mitros, J. P., Bartlett, J. A., Walters, J. D., Jia, H. P., Welsh, M. J., Casavant, T. L., and McCray, P. B., Jr. (2002) *Proc. Natl. Acad. Sci. U. S. A.* **99**, 2129–2133
26. Kim, C., Gajendran, N., Mittrucker, H. W., Weiwad, M., Song, Y. H., Hurwitz, R., Wilmanns, M., Fischer, G., and Kaufmann, S. H. (2005) *Proc. Natl. Acad. Sci. U. S. A.* **102**, 4830–4835
27. Nguyen, T. X., Cole, A. M., and Lehrer, R. I. (2003) *Peptides* **24**, 1647–1654
28. Selsted, M. E. (2004) *Curr. Protein Pept. Sci* **5**, 365–371
29. Tang, Y. Q., Yuan, J., Osapay, G., Osapay, K., Tran, D., Miller, C. J., Ouellette, A. J., and Selsted, M. E. (1999) *Science* **286**, 498–502
30. Leonova, L., Kokryakov, V. N., Aleshina, G., Hong, T., Nguyen, T., Zhao, C., Waring, A. J., and Lehrer, R. I. (2001) *J. Leukoc. Biol.* **70**, 461–464
31. Cole, A. M., Hong, T., Boo, L. M., Nguyen, T., Zhao, C., Bristol, G., Zack, J. A., Waring, A. J., Yang, O. O., and Lehrer, R. I. (2002) *Proc. Natl. Acad. Sci. U. S. A.* **99**, 1813–1818
32. Wu, Z., Powell, R., and Lu, W. (2003) *J. Am. Chem. Soc.* **125**, 2402–2403
33. Banks, D. J., Barnajian, M., Maldonado-Arocho, F. J., Sanchez, A. M., and Bradley, K. A. (2005) *Cell Microbiol.* **7**, 1173–1185
34. Lehrer, R. I., Rosenman, M., Harwig, S. S., Jackson, R., and Eisenhauer, P. (1991) *J. Immunol. Methods* **137**, 167–173
35. Cohn, E. J., and Edsall, J. T. (1943) in *Proteins, Amino Acids and Peptides as Ions and Dipolar Ions* (Cohn, E. J., and Edsall, J. T., eds) pp. 374–377, Reinhold Publishing Corporation, New York
36. Morris, G. M., Goodsell, D. S., Halliday, R. S., Huey, R., Hart, W. E., Belew, R. K., and Olson, A. J. (1998) *J. Comput. Chem.* **19**, 1639–1662
37. Solis, F. J., and Wets, R. J. B. (1981) *Math. Operation Res.* **6**, 19–30
38. Pannifer, A. D., Wong, T. Y., Schwarzenbacher, R., Renatus, M., Petosa, C., Bienkowska, J., Lacy, D. B., Collier, R. J., Park, S., Leppla, S. H., Hanna, P., and Liddington, R. C. (2001) *Nature* **414**, 229–233
39. Turk, B. E., Wong, T. Y., Schwarzenbacher, R., Jarrell, E. T., Leppla, S. H., Collier, R. J., Liddington, R. C., and Cantley, L. C. (2004) *Nat. Struct. Mol. Biol.* **11**, 60–66
40. Shoop, W. L., Xiong, Y., Wiltsie, J., Woods, A., Guo, J., Pivnichny, J. V., Felcetto, T., Michael, B. F., Bansal, A., Cummings, R. T., Cunningham, B. R., Friedlander, A. M., Douglas, C. M., Patel, S. B., Wisniewski, D., Scapin, G., Salowe, S. P., Zaller, D. M., Chapman, K. T., Scolnick, E. M., Schmatz, D. M., Bartizal, K., MacCoss, M., and Hermes, J. D. (2005) *Proc. Natl. Acad. Sci. U. S. A.* **102**, 7958–7963
41. Vriend, G. (1990) *J. Mol. Graph.* **8**, 52–56
42. Mani, R., Buffy, J. J., Waring, A. J., Lehrer, R. I., and Hong, M. (2004) *Biochemistry* **43**, 13839–13848
43. Cornell, W. D., Bayli, C. I., Gould, I. R., Merz, K. M. J., Ferguson, D. M., Spellmeyer, D. C., Fox, T., Caldwell, J. W., and Kollman, P. A. (1995) *J. Am. Chem. Soc.* **117**, 5179–5197
44. Stote, R. H., and Karplus, M. (1995) *Proteins* **23**, 12–31
45. Kokryakov, V. N., Harwig, S. S., Panyutich, E. A., Shevchenko, A. A., Aleshina, G. M., Shamova, O. V., Korneva, H. A., and Lehrer, R. I. (1993) *FEBS Lett.* **327**, 231–236
46. Schmidt, M. W., Baldrige, K. K., Boat, J. A., Elbert, S. T., Gordon, M. S., Jensen, J. H., Koseki, S., Matsunaga, N., Nguyen, K. A., Su, S. J., Windus, T. L., Dupuis, M., and Montgomery, J. A. (1993) *J. Comput. Chem.* **14**, 1347–1363
47. Trabi, M., and Craik, D. J. (2002) *Trends Biochem. Sci.* **27**, 132–138
48. Mulvenna, J. P., Wang, C., and Craik, D. J. (2006) *Nucleic Acids Res.* **34**, D192–D194
49. Craik, D. J. (2006) *Science* **311**, 1563–1564
50. Wang, W., Cole, A. M., Hong, T., Waring, A. J., and Lehrer, R. I. (2003) *J. Immunol.* **170**, 4708–4716
51. Leikina, E., Delanoe-Ayari, H., Melikov, K., Cho, M. S., Chen, A., Waring, A. J., Wang, W., Xie, Y., Loo, J. A., Lehrer, R. I., and Chernomordik, L. V. (2005) *Nat. Immunol.* **6**, 995–1001
52. Yasin, B., Wang, W., Pang, M., Cheshenko, N., Hong, T., Waring, A. J., Herold, B. C., Wagar, E. A., and Lehrer, R. I. (2004) *J. Virol.* **78**, 5147–5156
53. Chong-Cerrillo, C., Selsted, M. E., Peterson, E. M., and de la Maza, L. M. (2003) *J. Pept. Res.* **61**, 237–242
54. Tran, D., Tran, P. A., Tang, Y. Q., Yuan, J., Cole, T., and Selsted, M. E. (2002) *J. Biol. Chem.* **277**, 3079–3084
55. Demchick, P., and Koch, A. L. (1996) *J. Bacteriol.* **178**, 768–773
56. Mayer-Scholl, A., Hurwitz, R., Brinkmann, V., Schmid, M., Jungblut, P., Weinrauch, Y., and Zychlinsky, A. (2005) *PLoS Pathog.* **1**, e23
57. Lehrer, R. I., and Ganz, T. (1992) *Ciba Found. Symp.* **171**, 276–290
58. Rice, W. G., Ganz, T., Kinkade, J. M., Jr., Selsted, M. E., Lehrer, R. I., and Parmley, R. T. (1987) *Blood* **70**, 757–765
59. Gidalevitz, D., Ishitsuka, Y., Muresan, A. S., Kononov, O., Waring, A. J., Lehrer, R. I., and Lee, K. Y. (2003) *Proc. Natl. Acad. Sci. U. S. A.* **100**, 6302–6307
60. Heller, W. T., Waring, A. J., Lehrer, R. I., Harroun, T. A., Weiss, T. M., Yang, L., and Huang, H. W. (2000) *Biochemistry* **39**, 139–145
61. Weiss, T. M., Yang, L., Ding, L., Waring, A. J., Lehrer, R. I., and Huang, H. W. (2002) *Biochemistry* **41**, 10070–10076
62. Buffy, J. J., Hong, T., Yamaguchi, S., Waring, A. J., Lehrer, R. I., and Hong, M. (2003) *Biophys. J.* **85**, 2363–2373
63. Buffy, J. J., Waring, A. J., Lehrer, R. I., and Hong, M. (2003) *Biochemistry* **42**, 13725–13734
64. Buffy, J. J., McCormick, M. J., Wi, S., Waring, A., Lehrer, R. I., and Hong, M. (2004) *Biochemistry* **43**, 9800–9812